

Hot-phonon temperature and lifetime in a biased $\text{Al}_x\text{Ga}_{1-x}\text{N}/\text{GaN}$ channel estimated from noise analysis

A. Matulionis,* J. Liberis, I. Matulionienė, and M. Ramonas
Semiconductor Physics Institute, A. Goštauto 11, Vilnius 2600, Lithuania

L. F. Eastman, J. R. Shealy, V. Tilak, and A. Vertiatchikh
Cornell University, 425 Philips Hall, Ithaca, New York 14853, USA

(Received 21 January 2003; revised manuscript received 13 May 2003; published 31 July 2003)

The short-time-domain gated radiometric microwave noise technique is developed for the investigation of hot phonons in a two-dimensional electron gas channel subjected to a strong electric field applied in the plane of electron confinement. Nominally undoped pseudomorphic $\text{Al}_{0.15}\text{Ga}_{0.85}\text{N}/\text{GaN}$ channels are considered in the field range where LO-phonon emission by hot electrons and hot LO-phonon disintegration are mainly responsible for the energy dissipation. At a 5 kV/cm electric field, the equivalent temperature of the emitted LO phonons reaches 590 and 460 K at 80 and 293 K ambient temperatures, respectively. The electrons and emitted LO phonons form a nonequilibrium electron–LO-phonon subsystem characterized by a temperature different from that of the remaining phonons. The LO-phonon lifetime for their disintegration into the acoustic and other phonons is 350 ± 100 fs; the lifetime is almost independent of the hot-phonon and ambient temperatures. The deduced value of the LO-phonon lifetime is used as an input parameter for Monte Carlo simulation of the hot-phonon effect on the two-dimensional electron transport in the biased channel, and a reasonable agreement with the experimental current-voltage characteristics is obtained.

DOI: 10.1103/PhysRevB.68.035338

PACS number(s): 63.20.Kr, 72.20.Ht, 72.70.+m

I. INTRODUCTION

Nitride two-dimensional electron gas (2DEG) channels are the most promising for high-power microwave applications.¹ Under standard conditions of operation, the electrons are heated by an electric field and an efficient dissipation of the excess energy is of primary importance for channel performance.² Different experimental techniques^{3–6} have been used to study hot-electron energy relaxation in nitride 2DEG channels. At a high bias, the main electron energy relaxation mechanism includes emission of longitudinal optical (LO) phonons, their disintegration into acoustic and other phonons, and energy transfer towards the heat sink located at some distance from the channel. The disintegration of the emitted LO phonons is known to be a bottleneck for the energy relaxation.⁷ As a result, the LO-phonon distribution in the channel is strongly displaced from thermal equilibrium.⁸ The estimated equivalent temperature of the emitted LO phonons—the hot-phonon temperature—is higher than the “lattice” temperature of the rest phonons.⁹ Of course, the lattice temperature in the channel also exceeds that of the remote heat sink held at ambient temperature.¹⁰ Finally, since the 2DEG density is high, the electrons have their own hot-electron temperature.¹¹

The Monte Carlo technique was applied to simulate hot-electron effects in AlGaIn/GaN .^{8,12} The calculated hot-electron energy relaxation time was found to saturate at high electric fields, and the saturation value depended on the LO-phonon lifetime with respect to the nonequilibrium LO-phonon disintegration into other phonon modes.⁸ The results of the simulation with hot-phonons taken into account were in a reasonable agreement with the experimental data.⁴ An experimental high-field value of 550 fs was reported for the AlN/GaN 2DEG channel.⁹

Hot phonons also manifested themselves during time-resolved Raman light scattering^{7,13} and laser-excited–probe¹⁴ experiments carried out on bulk GaN samples. For bulk GaN layers, the LO-phonon lifetime was estimated to decrease from 5 ps at 25 K down to values below 3 ps at 300 K.¹³ These values are essentially longer than the high-field values of the hot-electron energy relaxation time determined for AlGaIn/GaN and AlN/GaN 2DEG channels.^{4,8,9,11} Consequently, the LO-phonon lifetime estimated for GaN bulk samples from the Raman light scattering data¹³ are not applicable for 2DEG channels located in GaN. On the other hand, to our knowledge, time-resolved Raman light scattering experiments on hot phonons have not been carried out on nitride 2DEG channels. This paper aims to demonstrate that the hot-phonon lifetime in AlGaIn/GaN 2DEG channels can be extracted from microwave noise experiments.

II. SAMPLES

Two-electrode samples for noise temperature measurements were prepared from a nominally undoped $\text{Al}_{0.15}\text{Ga}_{0.85}\text{N}/\text{GaN}$ heterostructure with a 2DEG channel. Ohmic Ti/Al/Ti/Au electrodes were formed at 1100 K. The results will be presented for samples where the channel length $L = 12 \mu\text{m}$ and the electrode width $w = 120 \mu\text{m}$.

The heterostructure consisted of a 1- μm -thick GaN buffer layer on a 150- μm Al_2O_3 substrate; the buffer layer was overgrown with a pseudomorphic 25-nm layer of $\text{Al}_{0.15}\text{Ga}_{0.85}\text{N}$ and protected with a 33-nm layer of Si_3N_4 (for more details see Refs. 15 and 16). The conductive channel was located in the GaN layer close to the AlGaIn/GaN interface. A degenerate 2DEG was induced by spontaneous polarization and piezoelectric fields. The electron sheet density was estimated from Hall effect measurements: $n_{2D} = 5$

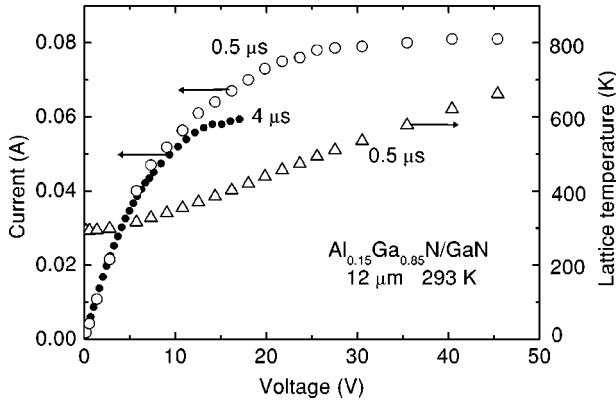


FIG. 1. Dependence of current on voltage for AlGaIn/GaN channel at 293 K ambient temperature. Voltage pulse duration is 4 μ s (solid circles) and 0.5 μ s (open circles). Open triangles stand for the lattice temperature at the end of a 0.5- μ s voltage pulse. $n_{2D} = 5 \times 10^{12} \text{ cm}^{-2}$, $\mu(293 \text{ K}) = 1200 \text{ cm}^2/(\text{V s})$, $L = 12 \text{ }\mu\text{m}$, and $w = 120 \text{ }\mu\text{m}$.

$\times 10^{12} \text{ cm}^{-2}$. The low-field mobility was $\mu(80 \text{ K}) = 3000 \text{ cm}^2/(\text{V s})$ and $\mu(293 \text{ K}) = 1200 \text{ cm}^2/(\text{V s})$.

Figure 1 illustrates the dependence of the current I on the voltage U applied along the 2DEG channel (the voltage drop on the contact resistances has been subtracted). The measurements were carried out for different durations of the pulsed voltage in order to show the effect of lattice heating on the current. Independently of the pulse duration, the effect was small at voltages $U < 7 \text{ V}$, but the effect became evident at higher voltages in the case of 4- μ s voltage pulses (Fig. 1, solid circles). The supplied heat was reduced 8 times when 0.5- μ s voltage pulses were applied (Fig. 1, open circles).

The lattice temperature was estimated from the time-dependent noise power measurements through backward extrapolation of the dependence on time after the voltage was switched off.^{17,18} Open triangles in Fig. 1 illustrate the lattice temperature under bias at the end of a 0.5- μ s voltage pulse.

III. HOT-ELECTRON TEMPERATURE

The 2DEG channels were subjected to a pulsed voltage applied parallel to the interface, and the microwave noise power was measured in the current direction. The gated modulation-type radiometric setup was used for the pulsed measurements.¹⁷ The hot-electron noise temperature was determined from the data on the emitted noise power. Sample mismatch and the contribution of noise sources outside the 2DEG channel (due to the contact resistance and microwave circuit elements) were taken into account in a way described elsewhere.⁴ The noise measurements were performed in the frequency band near 10 GHz where contributions due to generation-recombination noise and $1/f$ fluctuations were negligible. The thermal walkout due to lattice heating was minimized using 0.5- μ s pulses of bias voltage.

Figure 2 presents the dependence of the hot-electron noise temperature T_n on the applied voltage, measured at two ambient temperatures 80 and 293 K. Since the electron mobility is higher at 80 K, the electron heating is more efficient at the

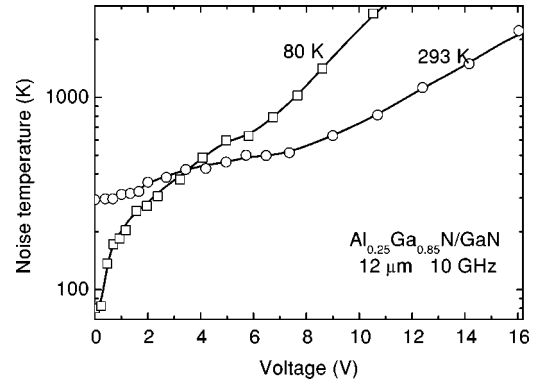


FIG. 2. Dependence of noise temperature at 10 GHz on voltage for the AlGaIn/GaN channel at two ambient temperatures: 80 K (squares) and 293 K (circles). Solid lines guide the eye. Voltage pulse duration is 0.5 μ s.

lower temperature. Thus, at $U > 3.5 \text{ V}$, the hot-electron temperature at 80 K becomes higher as compared with that at room temperature. Moreover, at a high voltage, the hot electrons penetrate into the AlGaIn barrier layer, and the hot-electron sharing between GaIn and AlGaIn layers causes additional noise.^{4,19,20} In our case, this source manifests itself at $U > 6 \text{ V}$ at 80 K ambient temperature and at $U > 8 \text{ V}$ at 293 K (Fig. 2). In the following we shall limit ourselves to the range of moderate voltages where the hot-electron sharing can be ignored.

The noise at moderate voltages is caused by two sources of hot-electron fluctuations: the main source is due to the hot-electron temperature T_e and the other source comes from fluctuations in the hot-electron temperature δT_e .¹¹ The hot-electron-temperature fluctuations cause current fluctuations if the electron mobility depends on the electron temperature—that is, if the current-voltage characteristics is not linear. The noise temperature can be expressed as a simple function of the nonlinearity and the electron temperature:¹¹

$$T_n = CT_e, \quad (1)$$

where the factor C is

$$C = \left[1 + \frac{T_e}{4(T_e - T_L)} \left(\frac{\sigma_{||}}{\tilde{\sigma}} - 1 \right)^2 \frac{\tilde{\sigma}}{\sigma_{||}} \right]. \quad (2)$$

Here $\sigma_{||} = dI/dU$ is the differential conductance, $\tilde{\sigma} = I/U$, and T_L is the lattice temperature. The factor C is unity if Ohm's law holds. For AlGaIn/GaN channels at electric fields below 4 kV/cm at 80 K ambient temperature, one has $C < 1.1$.¹¹ The current-voltage characteristics are almost linear in the field range of interest, and we shall assume $C \cong 1$.

IV. SUPPLIED POWER

Under bias, the electric power—the product of voltage and current—is supplied to the mobile electrons. Thus the supplied power per electron is

$$P_s = IU/N_e, \quad (3)$$

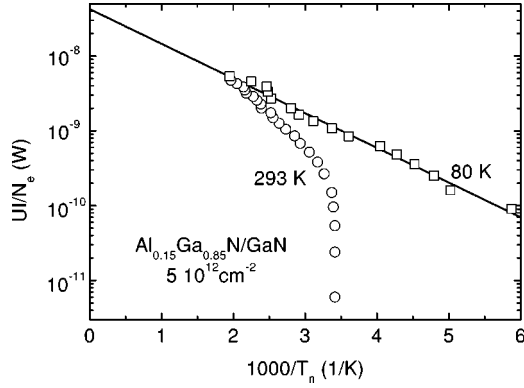


FIG. 3. The power supplied to the electron subsystem against the inverse noise temperature for AlGaN/GaN channel at two ambient temperatures: 80 K (squares) and 293 K (circles). Solid line is Eq. (4). $N_e = 7.2 \times 10^7$.

where N_e is the number of electrons in the 2DEG channel. The electron number can be estimated from the sheet electron density n_{2D} and the surface area A of the channel: $N_e = n_{2D}A$. In our case, $N_e = 7.2 \times 10^7$.

Figure 3 presents the supplied power as a function of the inverse noise temperature. The results at a room temperature (Fig. 3, circles) approach those at 80 K (squares) as the noise temperature T_n increases. The solid line in Fig. 3 is the empiric Arrhenius plot

$$P_s = \frac{\Delta \varepsilon}{\tau_{ph}} \exp\left(-\frac{\Delta \varepsilon}{k_B T_n}\right), \quad (4)$$

where $\Delta \varepsilon$ is the activation energy and τ_{ph} is the time constant. At an ambient temperature of 80 K (Fig. 3, squares), the supplied power obeys the exponential dependence (4) where $\Delta \varepsilon = 0.092$ eV and $\tau_{ph} = 350$ fs.

V. DISSIPATED POWER

Under a steady state, the supplied power P_s is balanced with the dissipated power P_d :

$$P_s = P_d. \quad (5)$$

In the electron temperature approach, the dissipated power is a function of the electron temperature. After Eqs. (5) and (1) where $C=1$ is assumed, the data of Fig. 3 can be interpreted as the dependence of the dissipated power on the inverse hot-electron temperature. It is evident that the power dissipation is the activated process controlled by the hot-electron temperature T_e . At $T_e < \Delta \varepsilon / k_B$ (Fig. 3), an average electron lacks energy for the emission of energy quanta equal to $\Delta \varepsilon$. The activation energy of the dissipation, $\Delta \varepsilon$, coincides with the LO-phonon energy $\hbar \omega$ [$\hbar \omega = 0.092$ eV in GaN (Ref. 21)]. Thus, the results of Fig. 3 confirm that the power is dissipated through LO-phonon emission by hot electrons.

This energy loss mechanism is known to dominate at electron temperatures exceeding certain value: for GaN, the critical temperature is 70 K at the lattice temperature of 1.5 K (Ref. 21). For AlGaN/GaN channels, the critical temperature

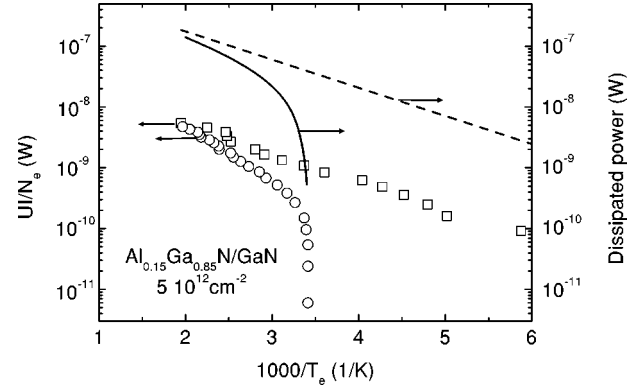


FIG. 4. Dependence of the power dissipated by the electrons vs the inverse hot-electron temperature at two lattice temperatures: dashed line is Eq. (6) valid at 80 K and solid line is Eq. (7) where the equilibrium phonon-state occupancy at 293 K is assumed. Symbols are for the supplied power at ambient temperatures: 80 K (squares) and 293 K (circles).

is near 160 K at the lattice temperature of 80 K (Ref. 5) and near 300 K at 293 K (Ref. 4).

At a low lattice temperature $T_L \ll \hbar \omega / k_B$, the mean power, dissipated by an electron through spontaneous emission of LO phonons, can be estimated as follows:

$$P_d = \frac{\hbar \omega}{\tau_{sp}} \exp\left(-\frac{\hbar \omega}{k_B T_e}\right), \quad (6)$$

where the exponential function accounts for the number of electrons able to emit optical phonons, $\hbar \omega$ is the LO-phonon energy (the energy lost in an event of emission), and $1/\tau_{sp}$ is the number of emission events per second (spontaneous emission rate). In GaN, the spontaneous LO-phonon emission time constant $\tau_{sp} \approx 10$ fs.²¹

At room temperature, the equilibrium LO phonons are present, and the dissipated power depends on the phonon-state occupancy f_{ph} , which is neglected in Eq. (6). The net dissipated power includes spontaneous and stimulated LO-phonon emission and LO-phonon absorption:

$$P_d = (1 + f_{ph}) \frac{\hbar \omega}{\tau_{sp}} \exp\left(-\frac{\hbar \omega}{k_B T_e}\right) - f_{ph} \frac{\hbar \omega}{\tau_{sp}}. \quad (7)$$

Expressions (6) and (7) assume Boltzmann statistics for hot electrons. The effects of hot-electron degeneracy have been considered;⁸ a minor correction is applicable under the conditions of interest. Supposing that the corrections were essential the empiric relation (4) would not hold.

Figure 4 compares the calculated dissipated power with the experimental data on the supplied power. Equation (1) with $C=1$ is used to present the experimental results (symbols) against the inverse electron temperature. The dissipated power is estimated according to Eqs. (6) and (7) where $\hbar \omega = 0.092$ eV and $\tau_{sp} = 10$ fs. At 80 K, the equilibrium phonon-state occupancy is negligible, and the dissipated power is given by Eq. (6) (dashed line). Solid curve is Eq. (7) where the equilibrium 293 K phonon-state occupancy (f_{ph}^{eq}) is inserted.

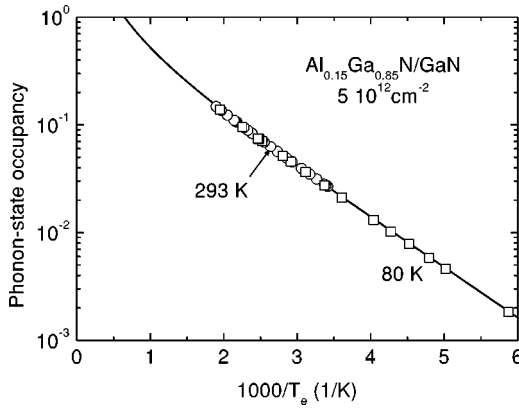


FIG. 5. Dependence on the inverse hot-electron temperature of occupancy of the selected LO-phonon states. The occupancy is a solution of the balance equation (8). The solid line is Eq. (9) where $T_e = T_{ph}$ is assumed.

Despite some similarity of the curves and the corresponding experimental points in Fig. 4, the disagreement is evident. This misfit would be even larger if Eqs. (6) and (7) took into account more energy loss mechanisms. On the other hand, the approach is based on Boltzmann rather than Fermi-Dirac statistics for the electrons. The interface phonons and the half-space phonons should be treated instead of bulk phonons. However, these modifications would not eliminate the essential misfit, and we state that the equilibrium occupancy of the LO-phonon states is not a solution of the energy balance equation (5).

VI. HOT PHONONS

Expressions (3) and (7) inserted into Eq. (5) lead to

$$IU/N_e = (1 + f_{ph}) \frac{\hbar\omega}{\tau_{sp}} \exp\left(-\frac{\hbar\omega}{k_B T_e}\right) - f_{ph} \frac{\hbar\omega}{\tau_{sp}}. \quad (8)$$

Let us solve Eq. (8) with respect to f_{ph} . The required experimental data are taken from Fig. 4; the values $\hbar\omega = 0.092$ eV and $\tau_{sp} = 10$ fs are used. In this way, an estimate is obtained for the average nonequilibrium occupancy of the selected LO-phonon states involved in the electron energy dissipation through LO-phonon emission (Fig. 5, symbols). An almost exponential dependence of the occupancy f_{ph} on the inverse electron temperature is obtained; the activation energy is $\Delta\varepsilon = 0.092$ eV [compare with Eq. (4)]. The obtained occupancy exceeds the equilibrium one: $f_{ph} > (f_{ph})_{eq}$. The term “hot phonons” is often used to emphasize the excess occupancy of the selected phonon states.²²

VII. HOT-PHONON TEMPERATURE

Let us interpret the nonequilibrium occupancy in terms of the equivalent hot-phonon temperature T_{ph} introduced according to the Bose-Einstein distribution

$$f_{ph} = \left[\exp\left(\frac{\hbar\omega}{k_B T_{ph}}\right) - 1 \right]^{-1}. \quad (9)$$

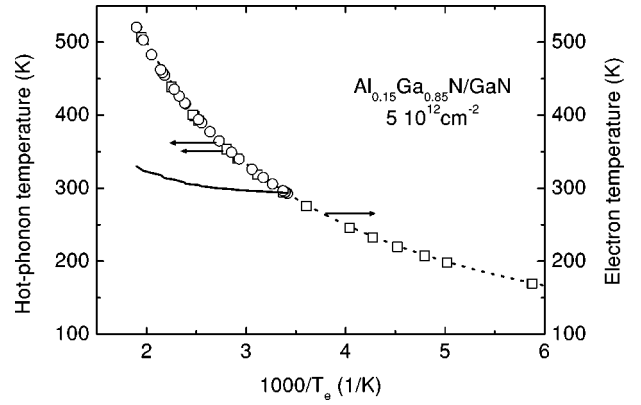


FIG. 6. Hot-phonon temperature (symbols) as a function of the inverse electron temperature at two ambient temperatures: 80 K (squares) and 293 K (circles). The dotted line is the electron temperature. The solid line is the lattice temperature at room temperature.

Figure 6 presents the hot-phonon temperature as a function of the inverse hot-electron temperature. Symbols stand for the data obtained according to Eq. (9) from the experimental results of Fig. 5. For a comparison, dotted line in Fig. 6 presents the hot-electron temperature. The lattice temperature measured at an ambient temperature of 293 K is also shown (Fig. 6, solid line).

Note that the hot-phonon temperature (Fig. 6, symbols) exceeds the lattice temperature (solid line). On the other hand, the hot-phonon temperature is insignificantly lower than that of the hot electrons (dotted line). This suggests one to assume $T_e \cong T_{ph}$ (see also Ref. 23). This approximate equality and Eq. (9) are used to plot the dependence of f_{ph} on the inverse temperature (Fig. 5, solid line). The comparison with the experimental data (Fig. 5, symbols) shows a good fit of the results. By the way, the experimental points (Fig. 5) are close to the straight line corresponding to Boltzmann statistics.

VIII. LO-PHONON LIFETIME

Figure 7 compares the dissipated power with the power exchanged between the hot-electron and the hot-phonon subsystems. The solid line in Fig. 7 shows the power received by the hot-phonon subsystem due to the spontaneous and stimulated emission of LO phonons—the first term of Eq. (7) where the nonequilibrium occupancy f_{ph} is determined by the hot-phonon temperature T_{ph} . The power returned by the hot-phonon subsystem back to the hot-electron subsystem (the LO-phonon reabsorption) is calculated as the second term of Eq. (7) (pentagons). The returned power is just slightly lower than the received one. The exchanged power does not change the energy of the electron–LO-phonon subsystem.

Under the steady state, the power P_s , supplied to the hot-electron subsystem, equals the power $(P_d)_{ph}$ dissipated by the hot-phonon subsystem into the lattice (Fig. 7, circles). The latter power is essentially lower as compared to the power exchanged inside the electron–LO-phonon subsystem.

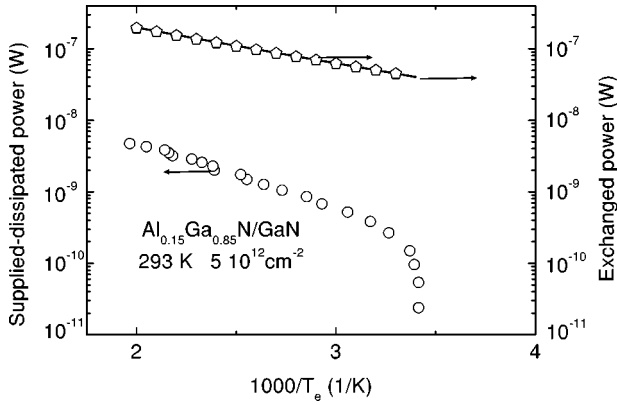


FIG. 7. Dependence, on the inverse hot-phonon temperature, of the power: received by the LO phonons from the hot electrons (solid line), returned by the LO phonons back to the hot electrons (pentagons), and dissipated by the LO phonons into the lattice (circles).

Consequently, at least two phonon lifetimes are needed to account for, respectively, the LO-phonon reabsorption and the LO-phonon disintegration into other phonons. Our experiment deals with the energy dissipation; that is, our goal is the LO-phonon disintegration lifetime.

Let us introduce the lifetime τ_{ph} as follows:

$$\left(\frac{\partial f_{ph}}{\partial t}\right)_{\text{disintegration}} = -\frac{f_{ph} - (f_{ph})_{eq}}{\tau_{ph}}. \quad (10)$$

The loss of the $\hbar\omega$ energy at the rate $[f_{ph} - (f_{ph})_{eq}]/\tau_{ph}$ causes the power dissipated by the LO-phonon subsystem to the lattice:

$$(P_d)_{ph} = \frac{\hbar\omega[f_{ph} - (f_{ph})_{eq}]}{\tau_{ph}}. \quad (11)$$

As mentioned, $P_s = (P_d)_{ph}$, and Eqs. (3) and (11) lead to the results for τ_{ph} presented in Fig. 8 (symbols). These experimental data show that the LO-phonon lifetime τ_{ph} is almost independent of the hot-phonon temperature T_{ph} in the temperature range below 500 K. The average value is $\tau_{ph} = 350 \pm 100$ fs. There is no evident dependence on the lattice tem-

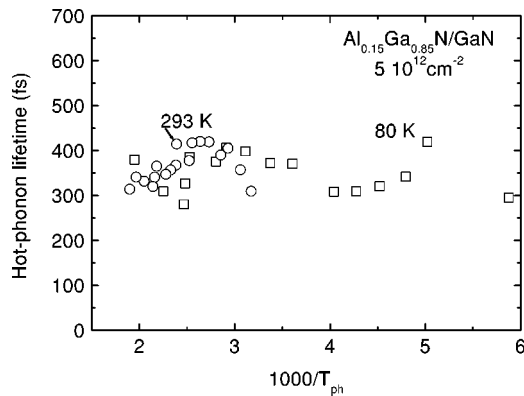


FIG. 8. Hot-phonon lifetime vs inverse hot-phonon temperature at two ambient temperatures: 293 K (circles) and 80 K (squares).

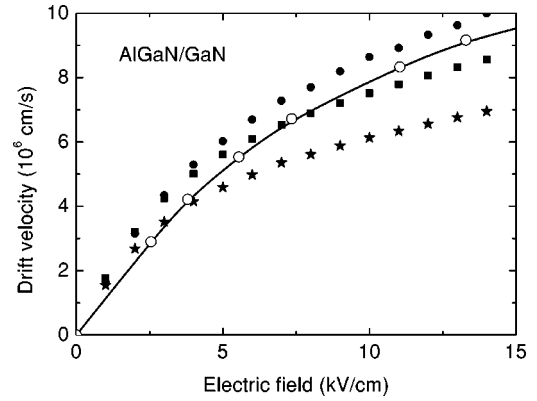


FIG. 9. Dependence of electron drift velocity on electric field. Experimental results are taken at the ambient temperature of 293 K (open circles) (Ref. 24). Monte Carlo data correspond to the lattice temperature of 300 K (solid symbols) for different hot-phonon lifetimes: 350 fs (solid circles), 1 ps (squares), and 3 ps (stars). The solid line guides the eye.

perature as well (Fig. 8). The hot-phonon lifetime values are close to the time constant entering the empiric relation (4).

IX. MONTE CARLO SIMULATION

The effect of the hot-phonon lifetime on the 2DEG transport is treated through semiclassical Monte Carlo simulation of electron motion in a biased channel. The model takes into account electron-phonon scattering, 2DEG degeneracy, and the nonequilibrium phonon distribution. The polar scattering of electrons by LO phonons takes into account screening of the phonon potential. The inelastic electron-acoustic-phonon interaction is treated in piezoelectric and deformation potential approaches. The LO-phonon lifetime is introduced to reach the steady-state distribution of hot phonons. The model and the technique are described elsewhere.⁸

Figure 9 presents the results of the simulation obtained for three fixed values of the LO-phonon lifetime (solid symbols). The calculated electron drift velocity is higher if the hot-phonon lifetime is shorter. In this case, the hot-phonon number is lower and the hot-phonon effect on the electron scattering is weaker. Open circles stand for the drift velocity estimated according to $v_{dr} = I/(en_{2D}w)$ where the current I is measured for 3-ns voltage pulses—that is, under conditions of fixed lattice temperature of the channel.²⁴ The experimental drift velocity is close to the calculated one for $\tau_{ph} = 350$ fs.

X. DISCUSSION

The main result is the LO-phonon lifetime. The same value of $\tau_{ph} \approx 350$ fs follows from a simple analysis of the electron-LO-phonon interaction (Fig. 8) and directly from the empiric relation (4) applied to the experimental data at 80 K (Fig. 3, squares) without considering the interaction in detail. Evidently, three conclusions follow: (i) the analysis is sound despite its simplicity and its weak points, (ii) the interpretation of the experimental data at 80 K is possible with-

out the analysis, and (iii) the analysis is indispensable at room temperature.

The interpretation of the experimental results has assumed that the hot-electron temperature can be introduced. The main argument for this approach is the strong inequality $\tau_e \gg \tau_{ee}$ where τ_e is the electron energy relaxation time and τ_{ee} is the interelectron relaxation time. In our case, this strong inequality holds since $\tau_e > \tau_{ph} \approx 350$ fs while the experimental results²⁵ suggest $\tau_{ee} \approx 44$ fs.

The LO phonons are assumed to be dispersionless. No mechanism for the LO-phonon disintegration into the rest phonons is considered. Only two parameters—the LO-phonon energy and the spontaneous emission time—are used within the simple analysis in order to account for the electron–LO-phonon interaction. The electrons are treated in terms of Boltzmann rather than Fermi-Dirac statistics. Support for the simple analysis is obtained through a Monte Carlo simulation that takes into account electron gas degeneracy, hot phonons, and considers the electron–LO-phonon scattering in all necessary details.

Despite its simplicity, the proposed analysis seems to be quite useful. It gives clear physical insight into the hot-electron–hot-phonon problem. It can be used for comparing the experimental results obtained for different 2DEG channels in different laboratories.

It is worth noting once more that no model of the electron–LO-phonon interaction is needed to obtain the activation energy $\Delta\varepsilon = 0.092$ eV and the LO-phonon lifetime $\tau_{ph} = 350$ fs from the experimental data at a low lattice temperature (Fig. 3). The obtained activation energy $\Delta\varepsilon$ is close to the LO-phonon energy $\hbar\omega$, while the LO-phonon lifetime is close to the results presented in Fig. 8.

The time-resolved Raman light scattering data^{7,13} have been interpreted in terms of the LO-phonon lifetime. For GaN, the LO-phonon lifetime is found to depend on the lattice temperature.¹³ The obtained LO-phonon lifetime is an order of magnitude longer as compared with our data (Fig. 8). Moreover, our results show a weak if any dependence on the lattice temperature. Possible reasons for the disagreement could be as follows.

The lifetime might be longer in GaN as compared with that in the 2DEG channel because of configuration considerations. Indeed, some hot phonons can escape from the 2DEG channel, thus reducing the number of LO phonons that can

be reabsorbed by the confined electrons. The lattice mismatch and resultant strain in the considered pseudomorphic AlGaIn/GaN structure can modify the anharmonic properties of the lattice vibrations responsible for the LO-phonon disintegration into other phonon modes. Also, limitations due to momentum conservation are less severe for confined phonons. The wave vectors of the LO phonons, emitted by laser-photogenerated electrons and holes during time-resolved Raman experiments, might differ from the wave vectors of the LO phonons emitted by the electrons accelerated in the electric field. Thus, time-resolved Raman experiments with a 100–300 fs time resolution would be quite helpful if performed on biased 2DEG channels. However, to our knowledge, no other experimental data on the hot-phonon lifetime is available for an AlGaIn/GaN channel containing a 2DEG.

XI. SUMMARY

A microwave noise technique is developed for the investigation of hot-electron and hot-phonon energy dissipation in the AlGaIn/GaN 2DEG channel subjected to an electric field. The hot-phonon temperature is found to be almost equal to (slightly lower than) the hot-electron temperature. The non-equilibrium occupancy of the hot-phonon states involved in electron–LO-phonon scattering can be approximated by an exponential function of the inverse hot-electron temperature. The activation energy is 0.092 eV; this value is close to the LO-phonon energy in GaN. The phonon nonequilibrium occupancy is controlled by the LO-phonon lifetime, which is found to be $350 \text{ fs} \pm 100 \text{ fs}$; the lifetime is almost independent of the hot-phonon temperature and the lattice temperature. The obtained value for the LO-phonon lifetime exceeds considerably the time for spontaneous emission of an LO phonon by a high-energy electron: $\tau_{ph} \approx 350 \text{ fs} \gg \tau_{sp} \approx 10 \text{ fs}$. Because of the long lifetime, the LO-phonon disintegration is a bottleneck for electron energy dissipation.

ACKNOWLEDGMENTS

The authors have benefited from discussions with Professor Brian Ridley. The Cornell group acknowledges support from ONR Contract No. N00014-01-1-0300; the Vilnius group acknowledges support from ONR Award Nos. N00014-01-1-0828 and N00014-03-1-0558.

*Electronic address: matulionis@uj.pfi.lt

¹H. Morkoç, *Nitride Semiconductors and Devices* (Springer, Berlin, 1999), p. 257.

²L.F. Eastman, V. Tilak, V. Kaper, J. Smart, R. Thompson, B. Green, J.R. Shealy, and T. Prunty, *Phys. Status Solidi A* **194**, 433 (2002).

³K.J. Lee, J.J. Harris, A.J. Kent, T. Wang, S. Sakai, D.K. Maude, and J.-C. Portal, *Appl. Phys. Lett.* **78**, 2893 (2001).

⁴A. Matulionis, J. Liberis, L. Ardaravičius, M. Ramonas, I. Matulionienė, and J. Smart, *Semicond. Sci. Technol.* **17**, L9 (2002).

⁵N. Balkan, M.C. Arikian, S. Golden, V. Tilak, B. Schaff, and R.J. Shealy, *J. Phys.: Condens. Matter* **14**, 3457 (2002).

⁶N. Shigekawa, K. Shiojima, and T. Suemitsu, *J. Appl. Phys.* **92**,

531 (2002).

⁷K.T. Tsen, R.P. Joshi, D.K. Ferry, A. Botchkarev, B. Sverdlov, A. Salvador, and H. Morkoç, *Appl. Phys. Lett.* **68**, 2990 (1996).

⁸M. Ramonas, A. Matulionis, and L. Rota, *Semicond. Sci. Technol.* **18**, 118 (2003).

⁹A. Matulionis, J. Liberis, L. Ardaravičius, J. Smart, D. Pavlidis, S. Hubbard, and L.F. Eastman, *Int. J. High Speed Electron. Syst.* **12**, 459 (2002).

¹⁰S.A. Vitusevich, S.V. Danylyuk, N. Klein, M.V. Petrychuk, A.Yu. Avksentyev, V.N. Sokolov, V.A. Kochelap, A.E. Belyaev, V. Tilak, J. Smart, A. Vertiatchikh, and L.F. Eastman, *Phys. Status Solidi C* **0**, 401 (2003).

¹¹A. Matulionis, R. Katilius, J. Liberis, L. Ardaravičius, L.F. Eastman, J.R. Shealy, and J. Smart, *J. Appl. Phys.* **92**, 4490 (2002).

- ¹²T.-H. Yu and K. Brennan, *J. Appl. Phys.* **91**, 3730 (2002).
- ¹³K.T. Tsen, D.K. Ferry, A. Botchkarev, B. Sverdlov, A. Salvador, and H. Morkoç, *Appl. Phys. Lett.* **72**, 2132 (1998).
- ¹⁴C.-K. Sun, F. Vallée, S. Keller, J.E. Bowers, and S.P. DenBaars, *Appl. Phys. Lett.* **70**, 2004 (1997).
- ¹⁵O. Ambacher, B. Foutz, J. Smart, J.R. Shealy, N.G. Weimann, K. Chu, M. Murphy, A.J. Sierakowski, W.J. Schaff, L.F. Eastman, R. Dimitrov, A. Mitchell, and M. Stutzmann, *J. Appl. Phys.* **87**, 334 (2000).
- ¹⁶R. Dimitrov, M. Murphy, J. Smart, W. Schaff, J.R. Shealy, L.F. Eastman, O. Ambacher, and M. Stutzmann, *J. Appl. Phys.* **87**, 3375 (2000).
- ¹⁷H. Hartnagel, R. Katilius, and A. Matulionis, *Microwave Noise in Semiconductor Devices* (Wiley, New York, 2001), pp. 86–90.
- ¹⁸M. de Murcia, E. Richard, J.M. Perraudin, A. Boyer, A. Benvenuti, and J. Zimmermann, *Semicond. Sci. Technol.* **10**, 515 (1995).
- ¹⁹A. Matulionis and I. Matulionienė, in *Noise and Fluctuations Control in Electronic Devices*, edited by A. Balandin (American Scientific, Stevenson Ranch, CA, 2002), p. 249.
- ²⁰A. Matulionis, J. Liberis, L. Ardaravičius, M. Ramonas, T. Zubkute, I. Matulionienė, L.F. Eastman, J.R. Shealy, J. Smart, D. Pavlidis, and S. Hubbard, *Phys. Status Solidi B* **234**, 826 (2002).
- ²¹N.M. Stanton, A.J. Kent, A.V. Akimov, P. Hawker, T.S. Cheng, and C.T. Foxon, *J. Appl. Phys.* **89**, 973 (2001).
- ²²P. Kocevar, *Physica B & C* **88**, 155 (1985).
- ²³M. Artaki and P.J. Price, *J. Appl. Phys.* **65**, 1317 (1989).
- ²⁴L. Ardaravičius, A. Matulionis, J. Liberis, O. Kiprianovičius, M. Ramonas, L.F. Eastman, J.R. Shealy, and A. Vertiatchikh (unpublished).
- ²⁵A.F. Braña, C. Diaz-Paniaqua, F. Batallan, J.A. Garrido, E. Muñoz, and F. Omnes, *J. Appl. Phys.* **88**, 932 (2000).